0026-895X/89/030430-07$02.00/0

MOLECULAR PHARMACOLOGY, 36:430-436

Selectivity of Quinoxalines and Kynurenines as Antagonists of the Glycine Site on *N*-Methyl-D-aspartate Receptors

N. W. KLECKNER and R. DINGLEDINE

Department of Pharmacology, University of North Carolina, Chapel Hill, North Carolina 27599

Received April 6, 1989; Accepted June 20, 1989

SUMMARY

Xenopus oocytes injected with rat brain mRNA were used to identify and characterize the effects of compounds that are antagonists at both the glycine site on *N*-methyl-D-aspartate (NMDA) receptors and the quisqualate/kainate receptor. Oocytes were voltage-clamped at −60 mV and inward currents were measured at equilibrium following perfusion with agonists and antagonists. Application of 7-chlorokynurenic acid (7-Cl-Kyn) or 6,7-dichloro-3-hydroxy-2-quinoxaline carboxylic acid (6,7-diCl-HQC), each at 15 μM, produced a parallel shift to the right of the glycine concentration-response curve. Schild analysis indicated a K_B of 300 nM for 6,7-diCl-HQC and 350 nM for 7-Cl-Kyn. The slopes of the Schild plots were 1.01–1.02 in each case, suggesting that both compounds are competitive glycine antagonists. Both compounds also blocked the receptor mediating kainate-induced inward current. Schild analysis of 6,7-diCl-HQC (K_B = 3.0 μM, slope = 0.98) indicated competitive antagonism of kainate currents, but with a potency 10-fold lower than at the glycine site. 7-Cl-Kyn antagonized kainate-evoked currents (K_B = 14.1 μM), but the slope of the Schild regression was less than 1 (0.72 ± 0.11; $p < 0.05$). Thus, 7-Cl-kyn was approximately 40-fold more potent at the glycine site than at the receptor mediating kainate currents but is probably not entirely competitive at the latter receptor. Omission of the Cl groups from these antagonists drastically reduced activity at both glycine and kainate sites. 6,7-Dinitro- and 6-cyano-7-nitro-quinoxalinedione were both more potent antagonists of kainate than glycine, but substitution of Cl at the 6-position and especially the 6- and 7-positions increased potency at the glycine site. These results suggest that the glycine coagonist site of the NMDA receptor and the agonist binding site of the quisqualate/kainate receptor have some structural similarity. Halogenated derivatives of quinoxalines and kynurenines should be useful in evaluating the function of the glycine site in synaptic transmission mediated by NMDA receptors. In this regard we found that 7-Cl-kyn (5 and 15 μM) selectively attenuated NMDA receptor-mediated epileptiform bursts in the CA1 region of hippocampal slices perfused with zero-Mg medium, without reducing the amplitude of the primary population spike. This block could be overcome by 300 μM D-serine, which alone did not influence bursting. These results together indicate that the glycine site plays a role in epileptiform bursting mediated by NMDA receptors in adult rat hippocampus.

Of several binding sites on NMDA receptors, that activated by glycine has been the subject of intense recent interest. Glycine was initially found to potentiate the responses of NMDA receptor agonists in cultured neurons (1) and has been shown to be required for NMDA receptor activity in *Xenopus* oocytes (2, 3). Mayer *et al.* (4) recently reported that part of the observed potentiation by glycine was due to a relief from desensitization of the NMDA receptor. Glycine has also been shown to modulate the binding of uncompetitive NMDA receptor antagonists (5–8). This site, therefore, provides new opportunities for manipulating NMDA receptor function. An antagonist of this site could be used to define the role of the glycine site in synaptic transmission and might be effective against NMDA receptor-mediated neuropathologies (9–11), whereas currently available NMDA antagonists may not be clinically used (12, 13).

Several compounds with possible antagonist activity at the glycine site have been identified. Kynurenic acid and its more potent and selective derivative 7-Cl-kyn have been reported to compete with strychnine-insensitive [^{3}H]glycine binding (14). Glycine and D-serine can also overcome blockade of NMDA-mediated responses by these compounds in cultured neurons and hippocampal slices, suggesting that the kynurenines act at the glycine site (14–16). The reduction of NMDA responses by three quinoxalines, CNQX, DNQX, and 6,7-diCl-HQC, could also be overcome by raising the glycine concentration, but these

This work was supported by National Institutes of Health Grants NS-17771 and NS-23804, a grant from The Klingenstein Foundation (R.D.), and an Advanced Predoctoral Fellowship from the Pharmaceutical Manufacturers' Association Foundation (N.W.K.).

ABBREVIATIONS: NMDA, *N*-methyl-D-aspartate; AMPA, α-amino-3-hydroxy-5-methylisoxazole-4-propionic acid; MBS, modified Barth's solution; CNQX, 6-cyano-7-nitroquinoxaline-2,3-dione; DNQX, 6,7-dinitroquinoxaline-2,3-dione; 6,7-diCl-HQC, 6,7-dichloro-3-hydroxyquinoxaline-2-carboxylic acid; 7-Cl-kyn, 7-chlorokynurenate; 6-Cl-QX, 6-chloroquinoxaline-2,3-dione; 6,7-diCl-QX, 6,7-dichloroquinoxaline-2,3-dione; HQC, 3-hydroxyquinoxaline-2-carboxylic acid; HEPES, 4-(2-hydroxyethyl)-1-piperazineethanesulfonic acid; EGTA, [ethyleneglycol-bis-(β-aminoethyl ether)]tetraacetic acid.

compounds have significant activity against the kainate/quisqualate receptor as well (17–20). Although these quinoxaline and kynurenine derivatives appear to block the glycine site, it is unclear whether their effects are competitive and selective. We have used the *Xenopus* oocyte mRNA translation system to characterize six quinoxaline derivatives, plus kynurenic acid and 7-Cl-kyn, as antagonists of the glycine site on the NMDA receptor. Two of them, 6,7-diCl-HQC and 7-Cl-kyn, are potent competitive antagonists of this site. 7-Cl-kyn is also effective against bursting induced by low magnesium in the hippocampal slice preparation, suggesting a role for the glycine site in epileptiform bursting. All compounds tested interacted with both the glycine and kainate sites with only moderate selectivity, which suggests similarity in the receptor binding sites.

Materials and Methods

RNA extraction. RNA was prepared from rat brain by a variation of the Chirgwin method (21), as described by Verdoorn and Dingledine (22), and poly(A)$^+$ RNA was selected by one round of oligo(dT) cellulose chromatography (23). The final washed pellets were dissolved in sterile distilled water to a concentration of 0.8–1.2 mg of RNA/ml and were stored in single-use aliquots at −70°.

Oocytes. *Xenopus laevis* females were anesthetized with 0.12–0.16% tricaine methyl sulfonate. Lobes of ovary were removed through a small incision in the abdomen and placed in MBS (88 mM NaCl, 1 mM KCl, 2.4 mM sodium bicarbonate, 10 mM HEPES, 0.82 mM $MgSO_4$, 0.33 mM $Ca(NO_3)_2$, and 0.91 mM $CaCl_2$, supplemented with 0.01% each of penicillin and streptomycin). The ovary was cut into small pieces and incubated in Dispase (neutral protease, 1.5 mg/ml; Boehringer Mannheim Biochemicals) in MBS for about 1 hr, until oocytes began to dissociate from the ovary. Individual oocytes were placed in 100 mM sucrose in MBS until the oocyte began to shrink away from the follicle cell layer (1–10 min), and the follicle cells were then removed with jewelers forceps. Defolliculated oocytes were injected with 40–60 ng of poly(A)$^+$ RNA and cultured in MBS for 48 hr before electrophysiological experiments were begun. The oocytes remained viable for up to 7 days after removal from the ovary.

Electrophysiology. Oocytes were placed in a recording chamber and perfused continuously with MBS, in which the $MgSO_4$ was replaced with 0.55 mM $NaSO_4$, and an additional 0.5 mM $CaCl_2$ was added. Oocytes were impaled with two microelectrodes filled with 3 M CsCl and 10 mM EGTA, and were voltage-clamped (Axoclamp 2A; Axon Instruments) at a holding potential of −60 mV. Drugs were dissolved in MBS and were applied by switching the perfusion solution from MBS alone to MBS plus drug. Dose-response curves were constructed in the absence and presence of antagonist by applying sequentially increasing concentrations of agonist every 5 min, with a washout period between applications. Each drug application (1–2 min) was ended when an equilibrium current response for that concentration was reached. Current responses were recorded on FM tape and digitized on an IBM AT computer. The plateau drug-induced current was plotted against drug concentration, and the data were fit, by a nonlinear least squares curve-fitting program, to the logistic equation:

$$\text{Current} = \text{maximum current}/[1 + (EC_{50}/[\text{agonist}])^n] \quad (1)$$

where n represents the Hill coefficient and EC_{50} represents the concentration of agonist that elicits a half-maximal current response.

Schild analysis of antagonist potency was performed by the method described in Verdoorn *et al.* (19). Briefly, an agonist was applied by perfusion at three concentrations defining the linear portion of the dose-response curve and encompassing the EC_{50}, both in the absence and in the presence of three concentrations of antagonist. The dose ratio (DR) (the shift in the agonist EC_{50} produced by each concentration of antagonist) was calculated and the $\log(DR-1)$ was plotted against the logarithm of the antagonist concentration to produce the Schild plot. The slope of the resulting regression line should be equal to 1 for a competitive antagonist (24). The x-intercept is the pA_2, the negative logarithm of the dissociation constant (K_B) for the antagonist, which reflects the affinity of the antagonist for the binding site (24).

Hippocampal slice. Rat hippocampal slices were prepared and maintained as described previously (25). Epileptiform bursts of CA1 pyramidal cells were evoked by electrical stimulation of the Schaffer commissural pathway in slices perfused with zero-Mg medium, which unmasks an NMDA receptor component of the excitatory synaptic potential (26). Such bursts can be abolished by perfusion with D-2-amino-5-phosphonovaleric acid. The coastline burst index (27), which provides an objective measure of the intensity of bursts, was used to evaluate the effect of potential glycine site antagonists on evoked bursting. Measurements from 60 to 100 bursts were averaged in control conditions, then in the presence of 5 or 15 μM 7-Cl-kyn, and finally after adding 300 μM D-serine to the antagonist-containing medium. In the same experiments, the amplitude of the first evoked population spike was measured as an indicator of non-NMDA receptor activation. Data are expressed as a percentage of the control value.

Source of compounds. CNQX was a gift from T. Honore (Ferrosan Research Division, Denmark) and was later obtained from Tocris. All other quinoxalines and 7-Cl-kyn were obtained from Tocris. Kynurenate was obtained from Sigma Chemical Co. NMDA was obtained from Cambridge Research Biochemicals and glycine was from Pierce.

Results

Xenopus oocytes. We assessed the potency, competitiveness, and selectivity of antagonists of the glycine site on the NMDA receptor in *Xenopus* oocytes by construction of dose-response curves for glycine, NMDA, and kainate in the presence and absence of potential antagonists and, where appropriate, by Schild analysis. The compounds tested were quinoxalines, primarily those substituted in the 6- and 7-positions, and kynurenines. We first compared the ability of each compound to block inward currents produced by an EC_{80} of kainate (300 μM) or and EC_{85-90} of glycine (3 μM) plus a maximal concentration of NMDA (300 μM) (Fig. 1). With this procedure, approximately equieffective concentrations of both glycine and kainate were tested. The compounds most effective at inhibiting NMDA/glycine currents were chlorinated derivatives of the quinoxalines and kynurenines. 7-Cl-kyn (15 μM) reduced the current elicited by NMDA and glycine by 92 ± 3.9%, while reducing the current elicited by kainate by only 15.1 ± 3.2% (Fig. 1). 6,7-DiCl-HQC (15 μM) reduced the current elicited by NMDA plus glycine by 85 ± 0.8% and that elicited by kainate by 72 ± 2.1%. Its dione derivative, 6,7-diCl-QX, was slightly less effective against NMDA/glycine evoked currents but was significantly less effective against kainate currents than was 6,7-diCl-HQC. 6-Cl-QX was less effective than 6,7-diCl-HQC against glycine currents but was equally effective at the kainate site. For each of these compounds, when the NMDA/glycine current had an initial desensitizing phase, both the initial phase and the equilibrium current were blocked, although the initial phase was blocked to a greater extent (e.g., Figs. 2B and 3A).

The unhalogenated derivatives of these compounds were virtually ineffective at antagonizing either glycine or kainate currents, at a concentration of 15 μM. Kynurenate blocked only 16.6 ± 11.3 and 7.3 ± 5.8% of NMDA/glycine and kainate currents, respectively (Fig. 1). HQC was even less effective, blocking 3.8 ± 8.8 and 3.2 ± 10.4% of NMDA/glycine and kainate currents. In contrast to both of the above groups of compounds, CNQX and DNQX blocked kainate currents (97.0 ± 0.2 and 96.2 ± 1.6%, respectively) more effectively than

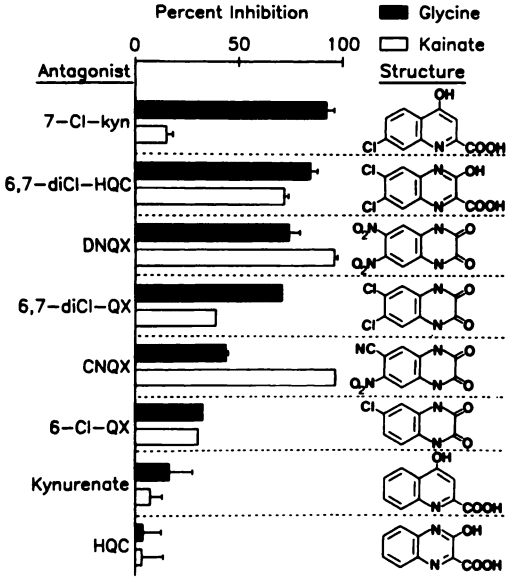

Fig. 1. Effectiveness of quinoxaline and kynurenic acid derivatives at antagonizing inward currents evoked by NMDA/glycine and kainate in *Xenopus* oocytes injected with rat brain mRNA. Oocytes were perfused with 3 μM glycine and 15 μM antagonist for at least 5 min before application of 300 μM NMDA or kainate in the presence of glycine and the antagonist. *Bars* represent the mean ± standard error of percentage of the NMDA/glycine- or kainate-induced current inhibited by each antagonist for three cells each, except for 6,7-diCl-QX and 6-Cl-QX where $n = 2$. Structures of each compound are given to the right of the corresponding bars.

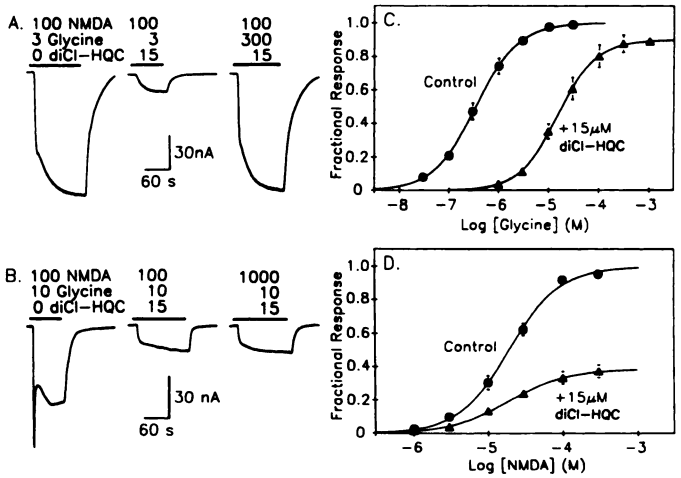

Fig. 2. 6,7-diCl-HQC antagonizes NMDA/glycine-induced currents by an interaction at the glycine site. A and B, The perfusion solution was changed to include NMDA and glycine, plus or minus the antagonist, 6,7-diCl-HQC (*diCl-HQC*), at the time indicated by the *horizontal bar*. The antagonist (15 μM) was perfused onto the oocyte for at least 5 min before drug application for the *center* and *right traces*. 6,7-diCl-HQC antagonism of the NMDA receptor was overcome by increasing the concentration of glycine (A) but not NMDA (B). Numbers represent the concentration of each drug in μM. C, Concentration-response curves for glycine generated in the absence and presence of 15 μM 6,7-diCl-HQC ($n = 3$). The NMDA concentration was 100 μM. 6,7-diCl-HQC caused a 45-fold parallel shift to the right of the glycine dose-response curve. The glycine EC_{50} was 0.35 (95% confidence interval, 0.23–0.55) μM in the absence of 6,7-diCl-HQC and 15.8 (10.2–24.5) μM in its presence. The Hill coefficients were 1.03 ± 0.03 and 1.15 ± 0.13. D, Concentration-response curves for NMDA in the absence and presence of 15 μM 6,7-diCl-HQC ($n = 3$). Glycine (10 μM) was present during NMDA applications. The antagonist decreased the maximum response of the NMDA dose-response curve by 65%. The EC_{50} was 19.1 (14.7–25.0) μM without antagonist and 20.4 (14.8–28.1) μM in the presence of antagonist. For both C and D, the *points* are the mean ± standard error of current (as a fraction of the maximum current in the absence of antagonist) for three cells. The *curves* represent the least squares fit of the data to the logistic equation, as described in Materials and Methods.

NMDA/glycine currents (44.1 ± 1.1 and 74.2 ± 5.3%), which is consistent with previous reports (17, 19, 28). We have previously shown that CNQX is a mixed competitive/noncompetitive antagonist of the glycine site (19).

The antagonism of the currents elicited by NMDA and glycine by 7-Cl-kyn and 6,7-diCl-HQC could be overcome by increasing the glycine concentration to 300 μM but not by increasing the NMDA concentration to 1 mM (Figs. 2A, 2B, and 3A). To characterize further the selectivity of these two antagonists, we determined their effects on full dose-response curves for glycine and kainate. Dose-response curves for glycine were shifted to the right in a parallel manner in the presence of either 15 μM 6,7-diCl-HQC (Fig. 2C) or 7-Cl-kyn (Fig. 3B). The magnitude of the shift was approximately 50-fold for each antagonist. In contrast, the maximum response of the NMDA dose-response curve was depressed by 6,7-diCl-HQC without a shift of the curve to the right (Fig. 2D). These results, taken together, are consistent with the interpretation that 6,7-diCl-HQC and 7-Cl-kyn act competitively at the glycine site on the NMDA receptor. Both compounds were less effective at shifting the dose-response curves for kainate. 6,7-DiCl-HQC (15 μM) shifted the kainate dose-response curve to the right by approximately 10-fold whereas the shift produced by 15 μM 7-Cl-kyn was only 2-fold (Figs. 4A and 5A).

To determine the relative potency of these two antagonists for the glycine and kainate sites and to further investigate the competitive nature of the antagonism, Schild analysis was performed. Dose-response curves for each agonist (glycine and kainate) were shifted to the right by increasing concentrations of each antagonist in a parallel manner (Figs. 3B, 4A, 5A, and 6A). As expected from the equivalent shifts in the glycine dose-response curves by 15 μM 6,7-diCl-HQC and 7-Cl-kyn, these compounds were approximately equipotent as antagonists of the glycine site. The K_B calculated from the Schild regression for 6,7-diCl-HQC was 0.30 μM and for 7-Cl-kyn was 0.35 μM (Figs. 3C and 6B). The slopes of the Schild regressions for 6,7-diCl-HQC and 7-Cl-kyn were 1.02 and 1.01, consistent with competitive antagonism against the glycine site (24).

The Schild analysis of these antagonists at the kainate site indicated that 6,7-diCl-HQC was 10-fold less potent for the kainate site than for the glycine site and 7-Cl-kyn was 40-fold less potent for the kainate site. The K_B values were 3.0 and 14 μM, respectively (Figs. 4B and 5B). A similar potency (K_B = 4.0 μM) has been reported elsewhere for 6,7-diCl-HQC antagonism of kainate-induced ^{22}Na efflux in preloaded brain slices from rat striatum (20). The slope of the Schild regression in oocytes was 0.98 ± 0.03 for 6,7-diCl-HQC, consistant with competitive antagonism. However, the Schild slope for 7-Cl-kyn antagonism of kainate currents was significantly less than 1 (0.72 ± 0.11; $p < 0.05$), indicating that its antagonism of this receptor is not entirely competitive.

To begin to assess the structural requirements of the quinoxalines for selective antagonism of the glycine site, the potency and selectivity of 6,7-diCl-HQC for antagonism of the glycine and kainate sites were compared with those of the nonchlorinated derivative HQC. Because 15 μM HQC was virtually

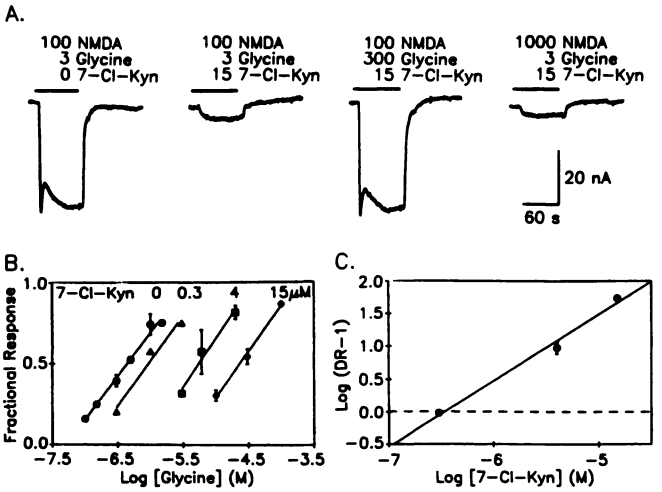

Fig. 3. 7-Cl-kyn antagonizes the NMDA/glycine-elicited current by an interaction with the glycine binding site. A, An mRNA-injected oocyte was perfused with MBS until, at the time indicated by the *horizontal bars*, the solution was changed to include NMDA and glycine in the absence or presence of 15 μM 7-Cl-kyn. 7-Cl-kyn was perfused onto the oocyte for at least 5 min before application of NMDA and glycine in the *right three traces*. Concentrations were in μM. 7-Cl-kyn antagonism of the NMDA receptor was overcome by increasing the concentration of glycine but not NMDA. B, Three-point dose-response curves for glycine were constructed in the absence and presence of the three concentrations of 7-Cl-kyn indicated above each curve. *Solid lines* are regression lines from which the EC_{50} values were calculated. The EC_{50} values for 0, 0.3, 4, and 15 μM antagonist were 0.45, 1.1, 5.3, and 23.1 μM, respectively. The *points* represent the mean ± standard error of current responses for three cells (except for 0.3 μM, which represents two cells). C, The Schild plot for 7-Cl-kyn antagonism of glycine was derived from the dose ratios calculated from the EC_{50} values from B. The pA_2 was 6.45, corresponding to a K_B of 0.35 μM, and the slope was 1.01. For both B and C, the *error bars* are smaller than the *symbol* size when not shown. *DR*, dose ratio.

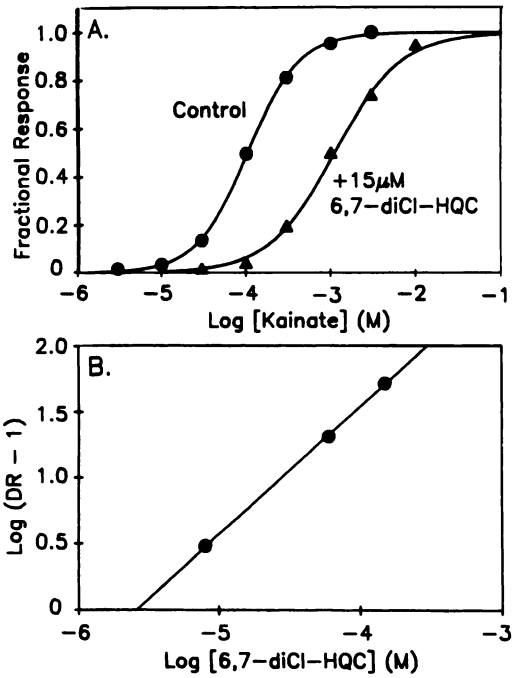

Fig. 4. 6,7-DiCl-HQC is a competitive antagonist of the receptor activated by kainate in oocytes. A, Dose-response curves for kainate were generated in the absence and presence of 15 μM 6,7-diCl-HQC. The dose-response curve was shifted 10.8-fold to the right in a parallel manner by 6,7-diCl-HQC. *Points* represent the mean ± current for five cells. Curves are the least squares fit of the data to the logistic equation. The kainate EC_{50} was 104 (94–115) μM in the absence of antagonist and 1110 (980–1270) μM in its presence. The Hill coefficients were 1.42 ± 0.01 in the absence and 1.11 ± 0.05 in the presence of antagonist. B, Schild analysis was performed by constructing three-point dose-response curves in the absence of 6,7-diCl-HQC and in the presence of 8, 60, and 150 μM 6,7-diCl-HQC ($n = 4$). The dose ratios (*DR*) were calculated from the EC_{50} of each curve and were plotted as the log(*DR*-1) against log[antagonist]. The slope of the regression line (0.98 ± 0.03) is consistent with competitive antagonism. The pA_2 of 6,7-diCl-HQC for the kainate site was 5.52 ± 0.06, corresponding to a K_B of 3.0 μM, indicating that the antagonist is 10-fold more potent for the glycine site than for the kainate site. The *points* represent the mean ± standard error for four cells. Standard errors were smaller than the *symbol* size in all cases.

ineffective at inhibiting currents elicited by 300 μM NMDA plus 3 μM glycine, or 300 μM kainate, dose-response curves for glycine and kainate were constructed in the absence and presence of 100 μM HQC. HQC caused a nearly parallel shift to the right of the glycine dose-response curve by only 7.4 ± 0.7-fold ($n = 3$) (Fig. 7A). These data predict a K_i for HQC antagonism of 15.6 μM, which is 45-fold less potent than the K_B of its chlorinated analog. HQC is even less effective at blocking the currents elicited by kainate in oocytes. HQC (100 μM) caused a parallel shift of the kainate dose-response curve to the right by only 2.5 ± 0.2-fold (Fig. 7B). The predicted K_i for HQC antagonism of kainate sites was 67 μM, which is 22-fold higher than the K_B of 3.0 μM for 6,7-diCl-HQC against kainate. HQC is, therefore, only 4-fold more effective against the glycine site than against the kainate site. The addition of the two chloro-groups to HQC increased the affinity of the antagonist for both the glycine site of the NMDA receptor and the kainate site and improved the selectivity of the antagonist for the glycine site.

Hippocampal slices. When 5 and 15 μM 7-Cl-kyn were applied to hippocampal slices that were perfused with medium containing no Mg^{2+}, the intensity of the NMDA receptor-mediated component of evoked bursting in the CA1 region was reduced in a dose-dependent manner (Fig. 8, *left*). The coastline burst index, which gives an objective measure of the intensity of bursting (27), was reduced in six slices by an average of 50 and 75% by 5 and 15 μM 7-Cl-kyn, respectively (Fig. 8, *right*). D-Serine (300 μM) reversed the effects of 15 μM 7-Cl-kyn. In contrast to the reduction of burst intensity, 7-Cl-kyn had no effect on the amplitude of the first population spike, which is probably mediated by synaptic activation of quisqualate receptors (29, 30). These data indicate that low micromolar concentrations of 7-Cl-kyn are selective for the glycine site on NMDA receptors in hippocampal slices as well as in oocytes. 6,7-DiCl-HQC (15 μM) had similar effects on evoked bursting in zero-Mg^{2+} medium but also caused a small reduction in the initial population spike amplitude.[1]

Discussion

Highly selective competitive antagonists are required to investigate the physiological role of the glycine modulatory site in NMDA receptor-mediated synaptic transmission. The principle findings of this study are that chloro-substituted quinoxalines and kynurenines are moderately selective glycine site antagonists, in that all compounds tested have, in addition, significant activity at the receptor that mediates kainate currents. The most selective compound, 7-Cl-kyn, was only 40-

[1] K. Kawasaki, unpublished observations.

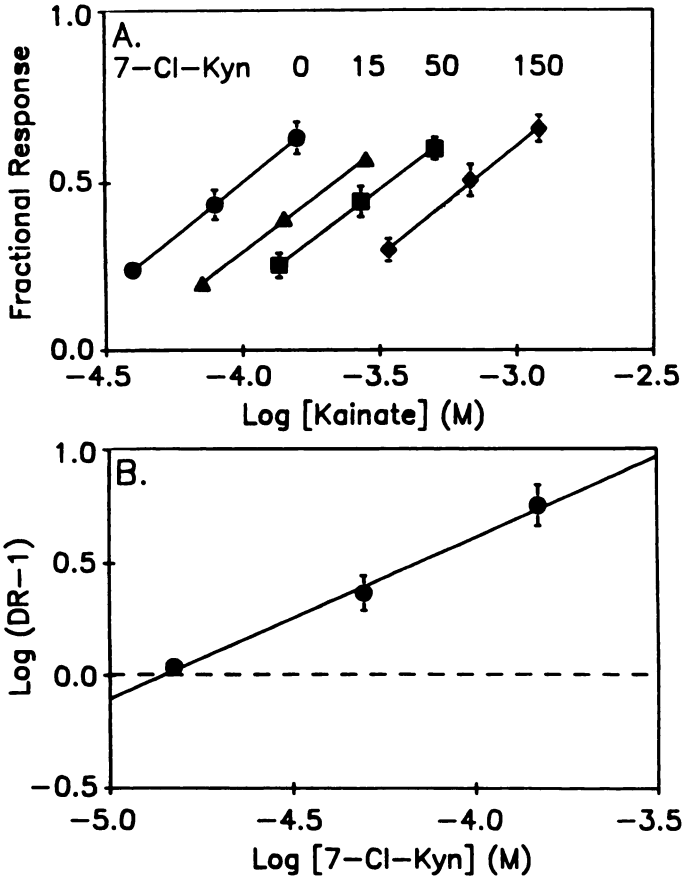

Fig. 5. 7-Cl-kyn antagonizes kainate-induced currents. A, Three-point dose-response curves were constructed for kainate in the absence of 7-Cl-kyn and in the presence of 15, 50, and 150 μM 7-Cl-kyn. The EC_{50} values calculated from the regression lines were 104, 217, 347, and 695 μM, respectively. The *points* represent the mean ± standard error of current from three cells. B, Schild plot of antagonist potency. The pA_2 was 4.85 ± 0.12, corresponding to a K_B of 14.1 μM, and the slope of the regression line was 0.72 ± 0.11. *Points* represent the mean ± standard error for three cells. *Error bars* are smaller than the *symbol* size when not shown. *DR*, dose ratio.

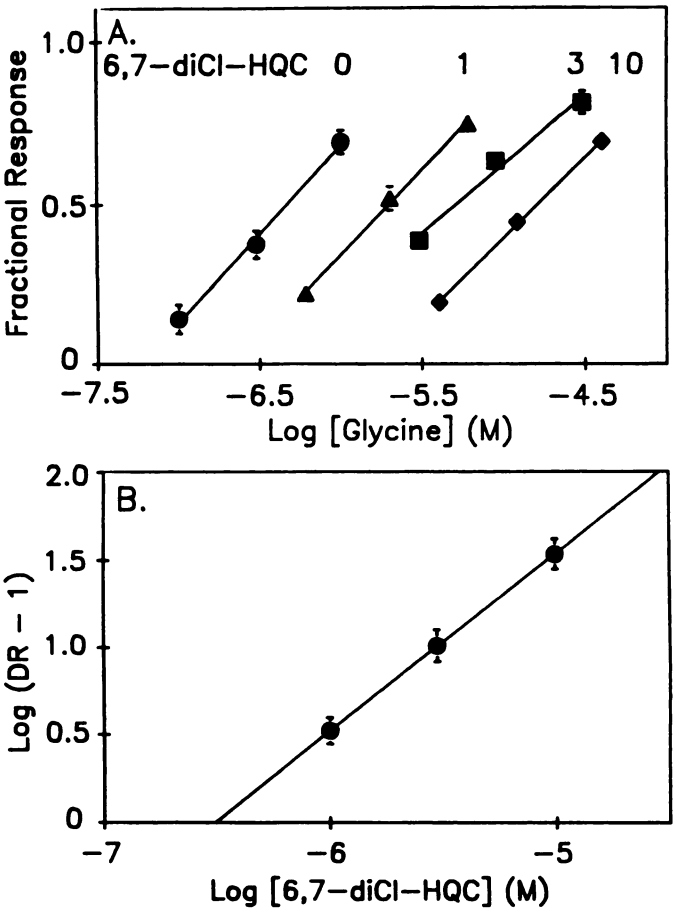

Fig. 6. Schild analysis indicating competitive antagonism of the glycine site on the NMDA receptor by 6,7-diCl-HQC. A, Three-point dose-response curves for glycine were generated in the absence of 6,7-diCl-HQC and in the presence of 1, 3, and 10 μM 6,7-diCl-HQC. The NMDA concentration was 100 μM throughout. The *points* represent the mean ± standard error of current as a fraction of the maximal current in the absence of antagonist for four cells. The EC_{50} values calculated from the regression lines were 0.47, 2.0, 5.2, and 16.4 μM, respectively. B, Schild plot for 6,7-diCl-HQC antagonism of glycine. The linear relationship between the points (r = 0.99), with the slope equal to 1.02 ± 0.06 (n = 3), suggests that the antagonism is competitive. The pA_2 of 6.52 ± 0.1 represents a K_B of 300 nM. *Points* represent the mean ± standard error for four cells. *Error bars* are smaller than the *symbol* size when not shown. *DR*, dose ratio.

fold more potent at the glycine site than at the kainate-activated receptor in *Xenopus* oocytes, making it moderately useful in physiological studies. Kemp *et al.* (14) found that 7-Cl-kyn displaced [^{3}H]glycine binding with an IC_{50} (0.56 μM) similar to our K_B for antagonism of NMDA/glycine currents (0.35 μM). However, their IC_{50} for 7-Cl-kyn displacement of [^{3}H]AMPA binding was 153 μM, contributing to an apparent 300-fold selectivity of 7-Cl-kyn for the glycine site. In our physiological experiments, the K_B of 7-Cl-kyn antagonism of kainate currents was 14 μM. The site that kainate activates in oocytes appears to correspond to an AMPA binding site in the brain (22), and the discrepancy between the binding and physiological data for 7-Cl-kyn antagonism of the quisqualate/kainate receptor may be due to antagonism of a high affinity AMPA binding site in the binding assays but a low affinity site in oocytes (31, 32). Halogenated indole-2-carboxylic acids also appear to antagonize NMDA/glycine-mediated currents at the glycine site, with approximately 40-fold selectivity for this site compared with the kainate/quisqualate receptor (33). However, these compounds are 40- to 50-fold less potent than 7-Cl-kyn and 6,7-diCl-HQC at the glycine site.

Another observation from this study is that a rapidly desensitizing component of NMDA/glycine-induced currents was more sensitive than the plateau current to inhibition by competitive glycine antagonists (e.g., Figs. 2B, and 3A). This initial peak was observed at high glycine concentrations (3 to 30 μM) but not at lower concentrations. It may, therefore, represent agonist-induced desensitization. Mayer *et al.* (4) found that, in voltage-clamped hippocampal neurons, the initial peak current was present at low glycine concentrations and increased with higher concentrations. The time constant of desensitization of the initial peak in their experiments (250 msec) was much faster than the decay time constant observed in our system (2–4 sec) and is, therefore, likely to represent a different component of the NMDA/glycine current that is unresolved in our slow perfusion system. The effect of high glycine concentration on NMDA receptor thus appears to be complex, in that activation is promoted, fast desensitization is reduced, and slow desensitization is increased.

Structural features for glycine antagonism. It is inter-

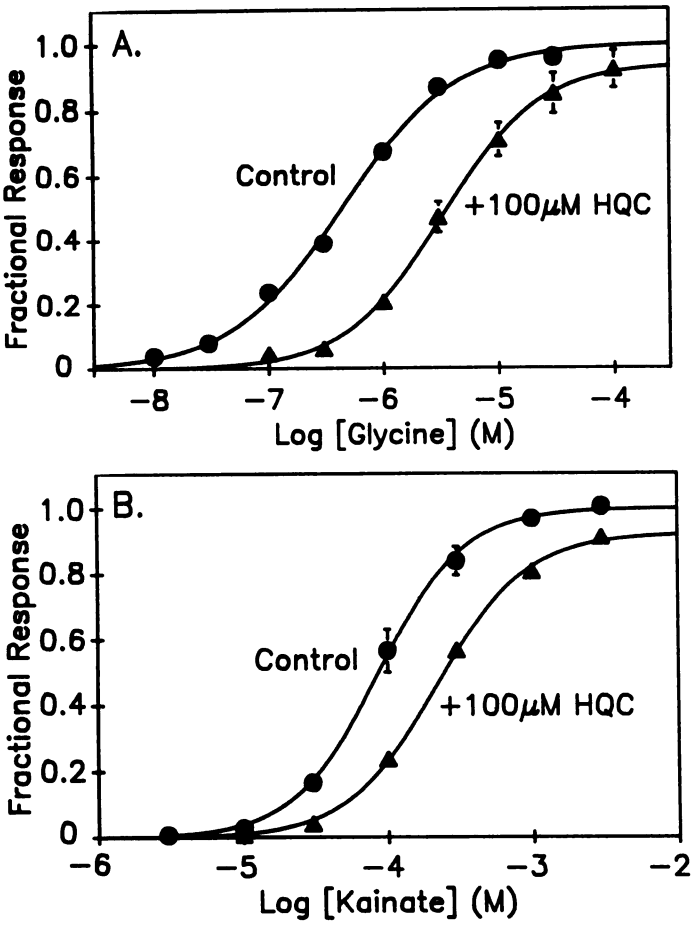

Fig. 7. HQC is a weak antagonist of glycine- and kainate-induced currents. A, Dose-response curves for glycine in the absence and presence of 100 μM HQC. HQC shifted the glycine dose-response curve to the right by 7.5-fold. The EC_{50} for glycine was 0.44 (0.35–0.56) μM in the absence and 3.25 (2.8–3.7) μM in the presence of 100 μM HQC, corresponding to an estimated K_i of 15.6 μM. The Hill coefficients were 0.9 ± 0.01 and 1.03 ± 0.03, respectively. B, Dose-response curves for kainate in the absence and presence of 100 μM HQC. HQC shifted the kainate dose-response curve to the right by 2.5-fold. The EC_{50} for kainate was 88.3 (61.8–126) μM in the absence and 219 (172–278) μM in the presence of 100 μM HQC. The estimated K_i for antagonism of kainate is 67 μM. The Hill coefficients were 1.48 ± 0.1 and 1.40 ± 0.04. In both A and B, the *points* represent the mean ± standard error for three cells each. The *curves* are the least squares fit of the data to the logistic equation. The K_i values for antagonism were calculated from the shift in the agonist EC_{50} produced by the antagonist, assuming competitive antagonism. A competitive antagonist shifts the EC_{50} by a factor of 1 + [antagonist]/K_i.

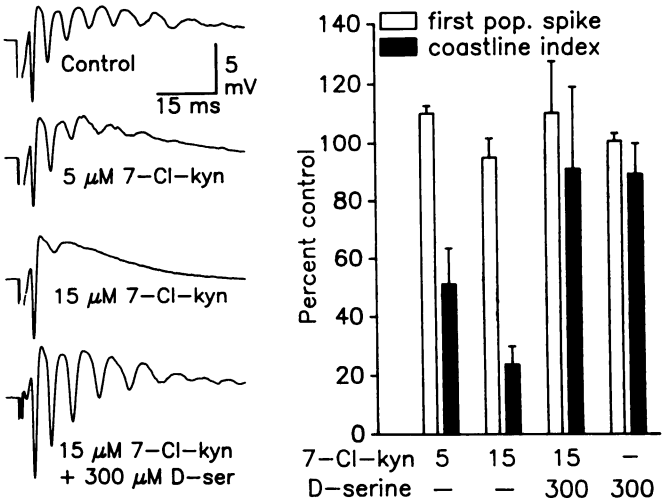

Fig. 8. 7-Cl-kyn reduced the NMDA receptor-mediated component of evoked bursts in hippocampal slices bathed in Mg^{2+}-free medium. A, Representative traces of evoked bursts of population spikes in the CA1 region of one slice bathed in Mg^{2+}-free medium in the absence and presence of 5 and 15 μM 7-Cl-kyn and 300 μM D-serine. Records are averages of four trials and were taken 30–45 min after changing solutions. B, Intensity of interictal bursts (coastline index) and the amplitude of the first population spike measured as a percentage of the control values in the absence of antagonist. *Bars* represent the mean ± standard error of measurements from 3–6 slices. 7-Cl-kyn at 5 and 15 μM reduced the coastline index by 50 and 75% without changing the magnitude of the first population spike. D-Serine (300 μM) reversed the antagonism of 15 μM 7-Cl-kyn, while having no effect on its own.

esting that all glycine site antagonists studied here are also antagonists of the quisqualate/kainate receptor. This suggests that there may be some structural similarity between the glycine site of NMDA receptors and the agonist binding site of quisqualate/kainate receptors. Lerma *et al.* (34) recently showed that kainate itself exerted a weak block of NMDA responses in oocytes; a prediction from the present study is that kainate blocks the glycine site rather than the NMDA binding site.

The addition of one or two chloro- groups to the basic kynurenine or quinoxaline structure (Fig. 1) dramatically improves the affinity of the compounds for the glycine site on the NMDA receptor, while improving the affinity for the kainate site to a lesser extent. The estimated K_B from Schild analysis for antagonism of the glycine site by 7-Cl-kyn was 0.35 μM (Fig. 3C), whereas high concentrations of kynurenate (100 μM) are required for substantial blockage of NMDA responses (16) (see also Fig. 1). In the quinoxaline series, a similar improvement in affinity for the glycine site occurs by adding two chloro- groups to HQC, from an estimated K_i of 15.6 μM for HQC to a K_B of 0.3 μM for 6,7-diCl-HQC. Halogenation of indole-2-carboxylic acid also improves the affinity for antagonism of the glycine site in primary cultures of rat visual cortex (33).

In addition, the *selectivity* of the antagonists for the glycine site improves with the addition of chloro- group(s). Kynurenate has poor selectivity for NMDA receptors over quisqualate/kainate receptors (Fig. 1) (14). 7-Cl-kyn, on the other hand, was 40-fold more potent at antagonizing the glycine site of NMDA receptors than the kainate site in oocytes. Likewise, HQC was only approximately 4-fold more potent against the glycine site, compared with kainate sites, whereas 6,7-diCl-HQC was 10-fold more potent at the glycine site. The addition of a second chloro- group to 6-Cl-QX also improved the selectivity of the antagonist for the glycine site (Fig. 1).

The improvement in affinity and selectivity for the glycine site by halogenation could be due to a number of factors. The substitution of the 6- and 7-positions with electronegative groups clearly improves affinity of the compounds, but for both glycine and kainate sites. Nitro- substitutions (CNQX and DNQX) confer selectivity at kainate receptors (Fig. 1) (17, 19), whereas chloro- groups confer selectivity at the glycine site. Substitution of the 6- and 7-positions with other electronegative groups, such as bromo- or fluoro- groups, might provide antagonists with an increased specificity for the glycine or kainate sites. 7-Cl-kyn has a dipole moment on the "lower" portion of the compound, which might contribute to its selectivity for the glycine site. However, 6-Cl-QX, which has a similar dipole, shows little selectivity (Fig. 1). A simple consid-

eration of charge distribution alone seems insufficient to explain the selectivity of these compounds.

Role of the glycine site in NMDA receptor-mediated epileptiform bursting. Glycine appears to be required for activation of NMDA receptors in *Xenopus* oocytes (2) and cultured hippocampal neurons (33) and in intact tissues the block of NMDA responses by kynurenic acid, 7-Cl-kyn, CNQX, DNQX, and HA-966 can be overcome by glycine (14, 16, 18, 35–37). These results demonstrate that the glycine site is operative in intact tissues, but a physiological role for glycine in synaptic transmission mediated by NMDA receptors is nearly unexplored. However, Larson and Beitz (38) recently demonstrated that intrathecal injection of glycine, acting at the NMDA receptor, can potentiate strychnine-induced seizures *in vivo* in adult rats. Here we present evidence that the glycine site on the NMDA receptor participates in epileptiform bursting mediated by synaptic activation of NMDA receptors in adult hippocampal slices. 7-Cl-kyn blocked the NMDA receptor-mediated component of bursts in a dose-dependent manner, without inhibiting the quisqualate receptor-mediated initial population spike (Fig. 8). The glycine site agonist, D-serine, at a concentration designed to give a near-maximal response in the presence of 15 μM 7-Cl-kyn in oocytes, overcame the block by 7-Cl-kyn in hippocampal slices. These results suggest that the glycine coagonist site of NMDA receptors plays an important role in epileptiform activity in adult differentiated neurons. Presumably the ambient glycine concentration is high enough to at least partially load its binding site.

References

1. Johnson, J., and P. Ascher. Glycine potentiates the NMDA response in cultured mouse brain neurons. *Nature (Lond.)* **325**:529–531 (1987).
2. Kleckner, N. W., and R. Dingledine. Requirement for glycine in activation of *N*-methyl-D-aspartate receptors expressed in *Xenopus* oocytes. *Science (Wash. D. C.)***241**:835–837 (1988).
3. Kushner, L., J. Lerma, R. S. Zukin, and M. V. L. Bennett. Coexpression of *N*-methyl-D-aspartate and phencyclidine receptors in *Xenopus* oocytes injected with rat brain mRNA. *Proc. Natl. Acad. Sci. USA* **85**:3250–3254 (1988).
4. Mayer, M. L., L. Vylicki, Jr., and J. Clements. Regulation of NMDA receptor desensitization in mouse hippocampal neurons by glycine. *Nature (Lond.)* **338**:425–427 (1989).
5. Bonhaus, D. W., B. C. Burge, and J. O. McNamara. Biochemical evidence that glycine allosterically regulates an NMDA receptor-coupled ion channel. *Eur. J. Pharmacol.* **142**:489–490 (1987).
6. Wong, E. H. F., A. R. Knight, and R. Ransom. Glycine modulates [^{3}H]-MK-801 binding to the NMDA receptor in rat brain. *Eur. J. Pharmacol.* **142**:487–488 (1987).
7. Snell, L. D., R. S. Morter, and K. M. Johnson. Glycine potentiates *N*-methyl-D-aspartate-induced [^{3}H]TCP binding to rat cortical membranes. *Neurosci. Lett.* **83**:313–317 (1987).
8. Reynolds, I. J., S. N. Murphy, and R. J. Miller. [^{3}H]MK-801 binding to the excitatory amino acid receptor complex from rat brain is enhanced by glycine. *Proc. Natl. Acad. Sci. USA* **84**:7744–7748 (1988).
9. Rothman, S. Synaptic release of excitatory amino acid neurotransmitter mediates anoxic neuronal death. *J. Neurosci.* **4**:1884–1891 (1984).
10. Simon, R. P., J. H. Swan, T. Griffiths, and B. S. Meldrum. Blockade of *N*-methyl-D-aspartate receptors may protect against ischemic damage in the brain. *Science (Wash. D. C.)* **226**:850–852 (1984).
11. Meldrum, B. S., M. J. Croucher, S. J. Czuczwar, J. F. Collins, K. Curry, M. Joseph, and T. W. Stone. A comparison of the anticonvulsant potency of (±)-2-amino-5-phosphonopentanoic acid and (±)-2-amino-7-phosphonoheptanoic acid. *Neuroscience* **9**:925–930 (1983).
12. Meldrum, B. S. Possible therapeutic applications of antagonists of excitatory amino acid neurotransmitters. *Clin. Sci.* **68**:113–122 (1985).
13. McNamara, J. O., R. D. Russell, L. Rigsbee, and D. W. Bonhaus. Anticonvulsant and antieptileptogenic actions of MK-801 in the kindling and electroshock models. *Neuropharmacology* **27**:563–568 (1988).
14. Kemp, J. A., A. C. Foster, P. D. Leeson, T. Priestly, R. Tridgett, L. L. Iversen, and G. N. Woodruff. 7-Chlorokynurenic acid is a selective antagonist at the glycine modulatory site of the *N*-methyl-D-aspartate receptor complex. *Proc. Natl. Acad. Sci. USA* **85**:6547–6550 (1988).
15. Kessler, M., M. Baudry, T. Terramani, and G. Lynch. Complex interactions between a glycine binding site and NMDA receptors. *Soc. Neurosci. Abstr.* **13**:760 (1987).
16. Watson, G. B., W. F. Hood, J. B. Monahan, and T. H. Lanthorn. Kynurenate antagonizes actions of *N*-methyl-D-aspartate through a glycine-sensitive receptor. *Neurosci. Res. Commun.* **2**:169–174 (1988).
17. Honore, T. G., S. N. Davies, J. Drejer, E. J. Fletcher, P. Jacobsen, D. Lodge, and F. E. Nielsen. Quinoxalinediones: potent competitive non-NMDA glutamate receptor antagonists. *Science (Wash. D. C.)* **241**:701–703 (1988).
18. Birch, P. J., C. J. Grossman, and A. G. Hayes. 6,7-Dinitro-quinoxaline-2,3-dion and 6-nitro-7-cyano-quinoxaline-2,3-dion antagonise responses to NMDA In the rat spinal cord via an action at the strychnine-insensitive glycine receptor. *Eur. J. Pharmacol.* **156**:177–180 (1988).
19. Verdoorn, T. A., W. Kleckner, and R. Dingledine. *N*-methyl-D-aspartate/glycine and quisqualate/kainate receptors expressed in *Xenopus* oocytes: antagonist pharmacology. *Mol. Pharmacol.* **35**:360–368 (1989).
20. Frey, P., C. Berney, P. L. Herrling, W. Mueller, and S. Urwyler. 6,7-Dichloro-3-hydroxy-2-quinoxalinecarboxylic acid is a relatively potent antagonist of NMDA and kainate receptors. *Neurosci. Lett.* **91**:194–198 (1988).
21. Chirgwin, J. M., A. E. Przybyla, R. J. MacDonald, and W. J. Rutter. Isolation of biologically active ribonucleic acid from sources enriched in ribonuclease. *Biochemistry* **18**:5294–5299 (1979).
22. Verdoorn, T. A., and R. Dingledine. Excitatory amino acid receptors expressed in *Xenopus* oocytes: agonist pharmacology. *Mol. Pharmacol.* **34**:298–307 (1988).
23. Aviv, H., and P. Leder. Purification of biologically active messenger RNA by chromatography on oligothymidylic acid-cellulose. *Proc. Natl. Acad. Sci. USA* **69**:1408–1412 (1972).
24. Arunlakshana, O., and H. O. Schild. Some quantitative uses of drug antagonists. *Br. J. Pharmacol.* **14**:48–57 (1959).
25. Dingledine, R., and S. J. Korn. γ-Aminobutyric acid uptake and the termination of inhibitory synaptic potentials in the rat hippocampal slice. *J. Physiol. (Lond.)* **366**:387–409 (1985).
26. Coan, E. J., and G. L. Collingridge. Magnesium ions block an *N*-methyl-D-aspartate receptor-mediated component of synaptic transmission in rat hippocampus. *Neurosci. Lett.* **53**:21–26 (1985).
27. Korn, S. J., L. Giacchino, N. L. Chamberlin, and R. Dingledine. Epileptiform burst activity induced by potassium in the hippocampus and its regulation by GABA-mediated inhibition. *J. Neurophysiol.* **57**:325–340 (1987).
28. Drejer, J., and T. Honore. New quinoxalines show potent antagonism of quisqualate response in cultured mouse cortical neurons. *Neurosci. Lett.* **87**:104–108 (1988).
29. Fletcher, E. J., D. Martin, J. A. Aram, D. Lodge, and T. Honore. Quinoxalinediones selectively block quisqualate and kainate receptors and synaptic events in rat neocortex and hippocampus and frog spinal cord *in vitro*. *Br. J. Pharmacol.* **95**:585–587 (1988).
30. Neuman, R. S., Y. Ben-Ari, M. Gho, and E. Cherubini. Blockade of excitatory synaptic transmission by 6-cyano-7-nitroquinoxaline-2,3-dione (CNQX) in the hippocampus *in vitro*. *Neurosci. Lett.* **92**:64–68 (1988).
31. Honore, T., J. Lauridsen, and P. Krogsgaard-Larsen. The binding of [^{3}H] AMPA, a structural analogue of glutamic acid, to rat brain membranes. *J. Neurochem.* **38**:173–178 (1982).
32. Olsen, R. W., O. Szamraj, and C. R. Houser. [^{3}H]AMPA binding to glutamate receptor subpopulations in rat brain. *Brain Res.* **402**:243–254 (1987).
33. Heuttner, J. E. Indole-2-carboxylic acid: a competitive antagonist of potentiation by glycine at the NMDA receptor. *Science* (Wash. D. C.) **242**:1611–1613 (1989).
34. Lerma, J., L. Kushner, D. C. Spray, M. V. L. Bennett, and R. S. Zukin. mRNA from NCB-20 cells encodes the *N*-methyl-D-aspartate/phencyclidine receptor: a *Xenopus* oocyte expression study. *Proc. Natl. Acad. Sci. USA* **86**:1708–1711 (1989).
35. Fletcher, E. J., and D. Lodge. Glycine reverses antagonism of *N*-methyl-D-aspartate (NMDA) by 1-hydroxy-aminopyrrolidone-2 (HA-966) but not by D-2-amino-5-phosphonovalerate (D-APV) on rat cortical slices. *Eur. J. Pharmacol.* **151**:161–162 (1988).
36. Shalaby, I., B. Chenard, and M. Prochniak. Glycine reverses 7-Cl-kynurenate block of glutamate neurotoxicity in cell culture. *Eur. J. Pharmacol.* **160**:309–311 (1989).
37. Foster, A. C., and J. A. Kemp. HA-966 antagonizes *N*-methyl-D-aspartate receptors through a selective interaction with the glycine modulatory site. *J. Neurochem.* **9**:2191–2196 (1989).
38. Larson, A. A., and A. J. Beitz. Glycine potentiates strychnine-induced convulsions: role of NMDA receptors. *J. Neurosci.* **8**:3822–3826 (1988).

Send reprint requests to: N. W. Kleckner, Dept. of Pharmacology, CB 7365 FLOB, University of North Carolina, Chapel Hill, NC 27599.